ELSEVIER

Polymer 41 (2000) 2059–2068

polymer

The mass transport of methanolic ferric chloride hexahydrate solution in poly(methyl methacrylate) and related optical properties

K.F. Chou, S. Lee*

Department of Materials Science, National Tsing Hua University, Hsinchu, Taiwan

Received 5 February 1999; received in revised form 24 May 1999; accepted 24 May 1999

Abstract

The mass transport of methanol mixed with ferric chloride hexahydrate ($FeCl_3 \cdot 6H_2O$) in poly(methyl methacrylate) (PMMA) and the related optical properties have been investigated. The ratio of $FeCl_3 \cdot 6H_2O$ to methanol in the solvent mixture is $X = 0.013$, 0.038 and 0.063 g/g. The mass transport is anomalous, which is a mixture of Case I with Case II transport. Both diffusion coefficient for Case I and velocity for Case II transport satisfy the Arrhenius equation. The activation energy of diffusion coefficient in Case I transport decreases with increasing X, but the trend for that of velocity in Case II transport is opposite. The mass transport is an endothermic process and satisfies the van't Hoff's plot. The heat of mixing increases with X. The transmittances of PMMA saturated with the solvent and solvent of methanol mixed with $FeCl_3 \cdot 6H_2O$ decrease with increasing X. The scattering intensity of the specimens after desorption is inversely proportional to the visible wavelength with an exponent, n, in the range from 1.02 to 3.25. The exponent is equal to 4 corresponding to the Rayleigh scattering. The wavelength dependence of scattering intensity is attributed to holes, the size of which is smaller than the visible wavelength, and to clouds. The holes and clouds in the solvent-treated specimen are observed by the scanning electron microscope and optical microscope. The deviation of the exponent n from 4 is due to the fractal dimension of hole and cloud. The FTIR spectra of specimens treated with solvent of different concentrations of $FeCl_3 \cdot 6H_2O$ are also studied.

Keywords: Ferric chloride hexahydrate; Transmission spectrum; Rayleigh scattering

1. Introduction

The incorporation of ferric chloride ($FeCl_3$) into polymers can induce pronounced changes in various properties of polymers. Rabek et al. [1] found that poly(ethylene oxide) (PEO), polyester poly(β-propiolactone) (PPL) and poly-(ether ester) poly(1,5-dioxepan-2-one) (PDXO) form coordinate complexes with $FeCl_3$. Under the UV irradiation, PEO–$FeCl_3$, PPL–$FeCl_3$ and PDXO–$FeCl_3$ complexes exhibit slow photo-degradation [1]. Tawansi et al. [2] studied the d.c. electrical resistivity and Curie point of polyvinylidene fluoride (PVDF) filled with $FeCl_3$. Rao and Chopra [3] observed that the electric conductivity of poly-(vinyl chloride) (PVC) films containing 4 wt.% of metallic salts such as $CoCl_2$, $CuCl_2$ or $FeCl_3$ increases to six orders of magnitude because the iron sites play the role of bridging for the transfer of electrons from one hopping center to another. Svorcik et al. [4] found that the $FeCl_3$ increases with a decrease of the PE sheet resistivity. Lindèn and Rabek [5] studied the chemical structure of poly(acrylic acid)-iron chloride (PAA–$FeCl_3$) gels and the mechanism of gel formation in water and hydrogen peroxide. The authors found that the stable and insoluble PAA–$FeCl_3$ gel can be applied to blocking of microscopic channels in tooth dentin. Mano et al. [6] investigated the mechanical, thermal and dynamic mechanical behaviors of PVC with various concentrations of $FeCl_3$. Stanke et al. [7] determined the oxidative crosslinking reaction of $FeCl_3$ with a polymer backbone consisting of poly(methyl methacrylate) (PMMA) with pyrrole-containing side groups. Bailey et al. [8] studied the growth mechanisms of iron oxide particles of different morphologies from the forced hydrolysis of ferric chloride solutions. Kawai et al. [9] analyzed the corrosion of iron in electrolytic anhydrous methanol solutions containing ferric chloride. The structure of non-aqueous ferric chloride solutions was studied using Mossbauer spectroscopy [10].

The large molecule transport in polymers is accounted for Case I, Case II and anomalous transport. The governing equation of Case I transport is the diffusion equation. The problems of diffusion equation with different boundary conditions were solved by Crank [11]. The solvent content of Case II transport is linearly proportional to time. Kwei and coworkers [12–16] were the first to propose a mathematical

* Corresponding author. Tel.: +886-3-571-8530; fax: +886-3-572-2366.
E-mail address: sblee@mse.nthu.edu.tw (S. Lee)

0032-3861/00/$ - see front matter
PII: S0032-3861(99)00373-0

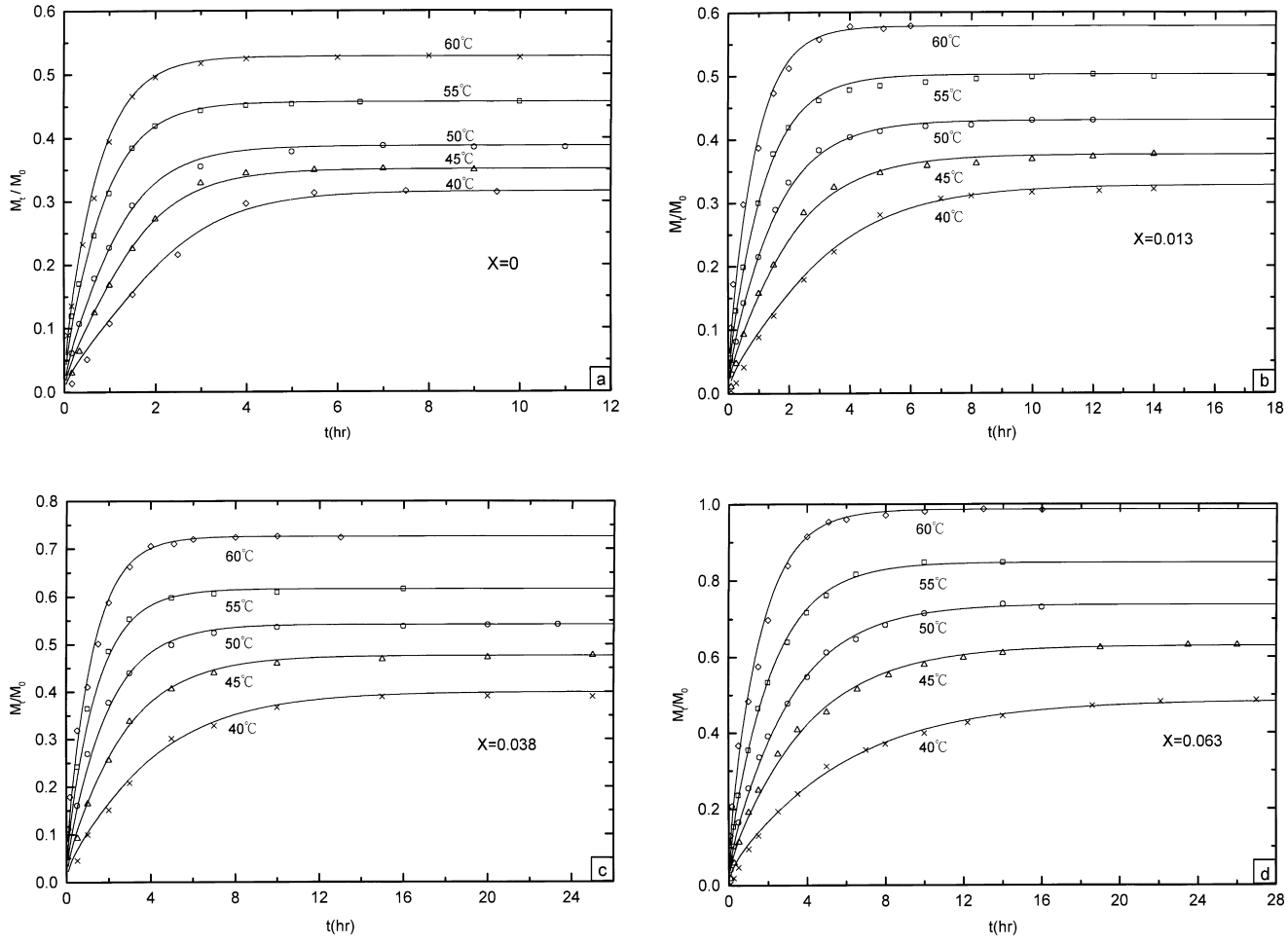

Fig. 1. The mass transport of methanol mixed with various concentrations of $FeCl_3 \cdot 6H_2O$ in PMMA at different temperatures: (a) $X = 0$ g/g; (b) 0.013 g/g; (c) 0.038 g/g and (d) 0.063 g/g. X denotes the ratios of $FeCl_3 \cdot 6H_2O$ in methanol.

model of anomalous diffusion in a semi-infinite medium, which is a combination of both Case I and Case II behaviors. Harmon et al. [17,18] modified the equation proposed by Kwei and coworkers and applied to the methanol transport in PMMA specimens of finite size. Svorcik et al. [4] analyzed the diffusion of $FeCl_3$ from water solution into ion-implanted PE using the Rutherford backscattering technique. These authors found that the ratio of atomic concentrations of Fe and Cl atoms in PE is about 2 and 3 for higher and lower implanted doses, respectively. So far, no literature has reported the mass transport of organic solvent mixed with ferric chloride in polymer in detail. It prompted us to investigate the diffusion behavior of methanol mixed with ferric chloride hexahydrate ($FeCl_3 \cdot 6H_2O$) in PMMA based on the Harmon's model.

Tyndall observed that the scattering intensity is inversely proportional to visible wavelength with exponent 4 [19]. The Tyndall effect was explained by Rayleigh scattering [19] that occurs when the particle size is smaller than the visible wavelength. The exponent 4 is due to the surface of particles which have a dimension of 2. However, Lin et al. [20] found that the exponent is smaller than 4 for the PMMA after methanol absorption, but they did not explain why the exponent is less than 4. In this paper, we explore the transmittance of PMMA when treated by methanol with various concentrations of $FeCl_3 \cdot 6H_2O$ and the effect of the ferric chloride hexahydrate addition on light scattering.

2. Experimental

PMMA with inherent viscosity 0.237 dl/g was obtained from the Du Pont Company in the form of a type-L Lucite cast acrylic sheet of thickness 6.35 mm. Specimens of $20 \times 6.35 \times 1.0$ mm^3 were cut from the sheet and ground using 800 and 1200 grid emery papers, followed by final polishing with 1 and 0.05 μm alumina slurries. The specimens were annealed at 95°C in air for 24 h and then furnace cooled to room temperature. $FeCl_3 \cdot 6H_2O$ and methanol were obtained from Hayashi Pure Chemical Industries and Shimakyu Chemicals Co., respectively. The solvent mixture was prepared with the ratio of $FeCl_3 \cdot 6H_2O$ methanol at 0.013, 0.038 and 0.063 g/g. The PMMA specimens and the solvent mixture were preheated separately to the same

Table 1
Diffusion coefficient (D) for Case I transport, velocity (v) for Case II transport and the equilibrium solvent content (ESC) in $FeCl_3 \cdot 6H_2O$/methanol/PMMA

T (K)	$FeCl_3 \cdot 6H_2O$/Methanol/ (g/g)	$D \times 10^8$ (cm^2/s)	$v \times 10^6$ (cm/s)	ESC (wt.%)
333	0	13.00	8.50	52.12
	0.013	8.90	6.20	57.81
	0.038	6.80	4.10	72.58
	0.063	5.20	3.10	98.71
328	0	8.00	7.10	45.73
	0.013	6.80	5.00	50.23
	0.038	5.50	3.40	61.63
	0.063	4.20	2.50	84.75
323	0	4.50	5.50	38.80
	0.013	4.70	3.80	43.06
	0.038	3.80	2.80	54.20
	0.063	2.80	1.90	73.84
318	0	2.60	4.30	34.98
	0.013	3.10	3.00	37.66
	0.038	2.50	2.00	47.64
	0.063	2.10	1.40	63.01
313	0	1.40	3.15	31.45
	0.013	1.80	2.20	32.82
	0.038	1.70	1.40	39.90
	0.063	1.50	1.00	54.82

elevated temperature. Then each specimen was immersed in the solvent mixture and kept at constant temperature in a thermostatted water bath at 40–60°C. The sorption study was conducted by periodically measuring the weight gain of the specimen until saturation. Specimens were weighed using an Ohaus analytical plus digital balance.

The specimen was saturated with the solvent mixture at 50°C and then desorbed for different periods at room temperature. Transmittance of solvent-treated specimen was measured in the wavelength range of 200–800 nm using a Hitachi U-3210/U-3240 spectrometer. The specimen of Fourier transform infrared (FTIR) spectra was saturated with the solvent and then desorbed for two weeks at room temperature. The infrared spectrum of solvent-treated specimen was measured in the range 500–2000 cm^{-1} by the attenuated total reflectance method using a Bomen DA8.3 FTIR spectrometer.

The specimen saturated with the solvent at 50°C and then desorption at room temperature was cleaved. The cleaved surfaces were observed using an Olympus BH-2 optical microscope and Joel 5200 scanning electron microscope (SEM). The cleaved surface of specimen was coated with gold for the observation of SEM. The opaque region appears in the cross-section of specimen saturated with the solvent of methanol mixed with 0.063 g/g $FeCl_3 \cdot 6H_2O$. Then the opaque region in the specimen after desorption for 7 days at room temperature was observed using an Olympus BH-2 optical microscope with transmitted light.

For the transition temperature study, a 10 mg cubic specimen immersed in solvent mixture with various concentrations of $FeCl_3 \cdot 6H_2O$ at 50°C for different periods was prepared. The specimen was quickly enclosed in a regular aluminum pan after removed from the water bath in order to avoid the escape of solvent from the specimen. Then the specimen was moved into a Seiko II differential scanning calorimeter immediately. The specimen was heated from room temperature to 200°C with a heating rate of 5°C/min. The inlet N_2 gas was operated with a flow rate of 40 ml/min. The change of heat flow with time was recorded.

3. Results and discussion

Fig. 1(a)–(d) shows the experimental data of mass transport for solvent of methanol mixed with different concentrations of $FeCl_3 \cdot 6H_2O$ at 40–60°C where M_0 ($= 0.123 \pm 0.003$ g) is the mass of virgin PMMA. Note that the definition of virgin specimen is the PMMA specimen prior to the solvent treatment. Because of the softening and large deformation, the transport experiment cannot be carried out for the concentration of $FeCl_3 \cdot 6H_2O$ greater than 0.063 g/g. These data can be analyzed using a mass transport model proposed by Harmon et al. [17]. Their model assumed that the transport behavior accounts for Case I, Case II and anomalous sorption. The characteristic parameters corresponding to Cases I and II are D for diffusion coefficient and v for velocity, respectively. D is due to the random walk of solvent molecules and v the stress relaxation of polymer chain. The specimen of thickness 2ℓ is free of solvent at the initial time and the concentration of solvent on both outer surfaces is maintained constant at all times. The weight gain of solvent, M_t, based on the one

dimension model is

$$\frac{M_t}{M_\infty} = 1 - 2\sum_{n=1}^{\infty} \frac{\lambda_n^2\left(1 - 2\cos\lambda_n \exp\left(-\frac{v\ell}{2D}\right)\right)}{\beta_n^4\left(1 - \frac{2D}{v\ell}\cos^2\lambda_n\right)} \exp\left(-\frac{\beta_n^2 Dt}{\ell^2}\right) \tag{1}$$

where λ_n is the nth positive root of the following equation:

$$\lambda_n = \frac{v\ell}{2D}\tan\lambda_n \tag{2}$$

$$\beta_n^2 = \frac{v^2\ell^2}{4D^2} + \lambda_n^2 \tag{3}$$

and M_∞ is the equilibrium weight of solvent. The solid lines in Fig. 1 are plotted using Eq. (1). It is found that the theoretical model is in good agreement with the experimental data for solvent with different concentrations of $FeCl_3{\cdot}6H_2O$. The values of D and v obtained from Fig. 1 are listed in Table 1. For $X > 0$, both D and v decrease with increasing concentration of $FeCl_3{\cdot}6H_2O$ at a given temperature. The values of D and v satisfy the Arrhenius equation:

$$D = D_0 \exp(-E_D/RT) \tag{4}$$

$$v = v_0 \exp(-E_v/RT) \tag{5}$$

where D_0 and v_0 are pre-exponent factors. E_D and E_v are activation energies of Case I and Case II transport, respectively. The values of E_D and E_v are calculated using Eqs. (4) and (5) and tabulated in Table 2. It is found that the

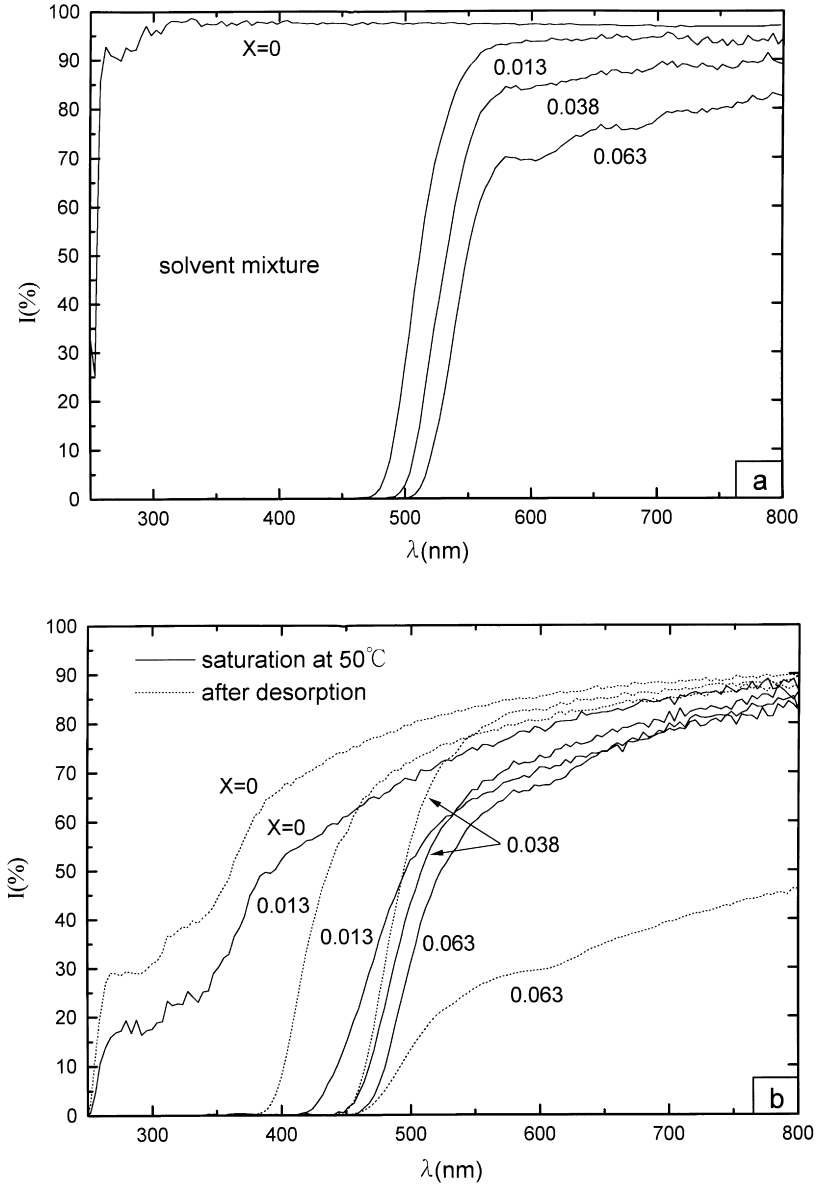

Fig. 2. Plot of transmittance versus wavelength λ in the range of 250–800 nm at 50°C (a) in the mixture of methanol and various concentrations of $FeCl_3{\cdot}6H_2O$; (b) in a specimen saturated with the solvent of different concentrations of $FeCl_3{\cdot}6H_2O$ before and after desorption.

Table 2
Activation energies of E_D and E_v for Case I and Case II transport and the heat of mixing ΔH

	$FeCl_3 \cdot 6H_2O$/methanol/ (g/g)			
	$X = 0$	0.013	0.038	0.063
E_D (kcal/mol)	23.88	17.03	15.21	13.61
E_v (kcal/mol)	10.64	11.06	11.44	12.15
ΔH (kcal/mol)	5.48	6.09	6.23	6.30

activation energy, E_D, of Case I diffusion decreases with increasing concentration of ferric chloride hexahydrate, but the trend for the activation energy of Case II diffusion is opposite. Comparing both activation energies of D and v, the effect of ferric chloride hexahydrate is more pronounced on Case I diffusion than on Case II diffusion.

The equilibrium solvent content, ESC, of the system is defined as the equilibrium weight of solvent in the specimen divided by the weight of virgin specimen. The values of ESC for various concentrations of $FeCl_3 \cdot 6H_2O$ at 40–60°C are listed in Table 1. The equilibrium solvent content increases with increasing temperature, irrespective of the addition of $FeCl_3 \cdot 6H_2O$. That is, the mass transport is an endothermic process. The equilibrium solvent content (ESC), satisfies the van't Hoff's equation:

$$(\mathrm{ESC}) = (\mathrm{ESC})_0 \exp(\Delta H/\mathrm{R}T), \quad (6)$$

where $(\mathrm{ESC})_0$ and ΔH are pre-exponent factor and heat of mixing, respectively. The values of ΔH were calculated using Eq. (6) and listed in Table 2. The heat of mixing increases with increasing concentration of $FeCl_3 \cdot 6H_2O$. At a given temperature, the equilibrium solvent content increases significantly with increasing concentration of $FeCl_3 \cdot 6H_2O$.

The addition of $FeCl_3 \cdot 6H_2O$ enhances the penetration of the solvent to PMMA. This implies that $FeCl_3 \cdot 6H_2O$ changes the interaction of methanol–methanol molecules or solvent–polymer molecules. Fig. 2(a) shows the transmission spectrum in the UV and visible regions of the solvent with different concentrations of $FeCl_3 \cdot 6H_2O$ at 50°C. The light rays in the measurement range almost penetrate through methanol, but those below 470 nm are completely absorbed by the solvent mixture. The cut-off wavelengths of solvent with different concentrations of $FeCl_3 \cdot 6H_2O$ are listed in Table 3 and shift to long wavelength side with more concentration of $FeCl_3 \cdot 6H_2O$. The ferric chloride hexahydrate is a coordinate compound, which may have more than one kind of ion-pairs or anions complex formed in the organic solvent, for example, FeS_6^{3+}, $FeClS_5^{2+}$, $FeCl_4^-$, $FeCl_2S_4^+$ and Cl^- [1,21,22], where S is the organic solvent molecule. After excited by light, these ion-pairs or anion complexes exhibited the charge transfer from ligand or solvent to metal center. The number of metal centers is reduced and the ligand or solvent is oxidized. As a result, an absorbed optical band induced by the charge transfer was observed. The light absorption arising from different ion-pairs and anion complexes is coupled to each other to form a broad band so that no isolated peak is present. The component with metal center of high oxidation state is produced in the solvent with large concentration of $FeCl_3 \cdot 6H_2O$. Therefore, the charge transfer process can be easily carried out, which is equivalent to a absorbed band extending to the range of a longer wavelength.

Table 3
Cut-off wavelengths (nm) for solvent with different concentrations (X) of $FeCl_3 \cdot 6H_2O$, and the measured wavelengths for PMMA saturated with the solvent and after desorption in air at room temperature

X (g/g)	Solvent	PMMA	
		Saturation	Desorption
0	< 250	250	249
0.013	472	416	384
0.038	490	448	448
0.063	504	460	460

The transmission spectrum of the specimen with saturated solvent is shown in Fig. 2(b) by solid lines. Compared to the transmission spectrum of solvent as shown in Fig. 2(a), the cut-off wavelength of transmittance shifts to the short wavelength side for each concentration of $FeCl_3 \cdot 6H_2O$. The interaction between solvent molecule and polymer chain makes a more stable state for the complex so that the higher energy of light is required to excite the photo-reaction. After desorption, there are some complex residues in the specimen. The weight percents of residue relative to that in the virgin specimen are 4.79, 6.56, 9.41 and 11.73% for $X = 0$, 0.013, 0.038 and 0.063 g/g, respectively. The charge transfer band is observed in Fig. 2(b) by the dashed lines. The cut-off wavelength for $X = 0.013$ shifts to the short wavelength side again, but those for $X = 0.038$ and 0.063 g/g remain the same. Some solvent complexes, which have a strong attractive force to polymer molecule, are left in the specimen treated with the solvent of low concentration of $FeCl_3 \cdot 6H_2O$. However, for the specimen treated with the solvent of high concentration of $FeCl_3 \cdot 6H_2O$, the force interaction between solvent and polymer chain is not a unique factor to prevent the escaping of solvent molecule. Further study will be made to identify the factors to affect the transmittance during the mass transport of methanol with high concentrations of $FeCl_3 \cdot 6H_2O$.

From the analysis of transmission spectra in the range of 250–800 nm, we find that $FeCl_3 \cdot 6H_2O$ interacts with methanol molecule to form complexes and disperses the intermolecular force of methanol molecules, like the hydrogen bond. The solvent complexes penetrated into PMMA also interact with polymer chains and form a more stable state. That is, the enhancement of solvent power [23] of the mixture of methanol with $FeCl_3 \cdot 6H_2O$ in PMMA is due to the interactions of $FeCl_3 \cdot 6H_2O$–methanol and solvent–polymer chains. The alternative interpretation is that the metal compound is provided a low energy pathway for

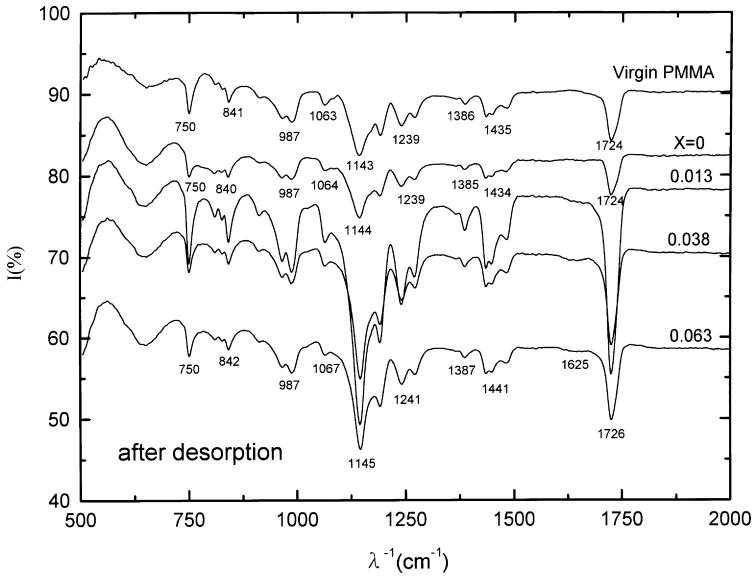

Fig. 3. FTIR spectra of specimens treated with solvent mixture of different concentrations of $FeCl_3 \cdot 6H_2O$ at 50°C after desorption, where I is the transmittance.

diffusion process either by the change of oxidation state or by the formation of appropriate intermediates, so that the activation energy is decreased [24].

The FTIR spectrum of the specimen treated with methanol mixed with different concentrations of $FeCl_3 \cdot 6H_2O$ is illustrated in Fig. 3. It sheds light on the interaction between solvent and polymer chains in an alternative way. The spectrum of virgin PMMA specimen shows the absorption peak of carbonyl group at 1724 cm^{-1}, and the vibration bands of methyl group at 1380–1500 cm^{-1} and methacrylate group at 1050–1230 cm^{-1}, respectively. Comparing the solvent-treated PMMA with virgin PMMA, some absorption peaks for the specimen treated with the solvents after desorption have a little shift and their intensities are reduced, but no new intense peak is observed. That is, the solvent complexes do not have covalent bonds to polymer chains. There are two obvious changes in the spectra. One is located at the absorption band between 1050–1145 cm^{-1}. The absorption peak on 1063 cm^{-1} for virgin PMMA shifts to 1067 cm^{-1} for $X = 0.063$. The energy for bond stretch is raised, and the shoulders of the two isolated peaks at 1063 and 1143 cm^{-1} in virgin PMMA become overlapped in the solvent-treated specimen due to coupling. This coupling effect arises from the interaction between the ester group of polymer and the solvent complex. The other change is located in the region between 1600 and 1700 cm^{-1}. The weak and broadened absorption band appears in the solvent-treated specimen, but no absorption band is observed in virgin PMMA. This weak and broadened band corresponds to the optical absorption of $FeCl_3 \cdot 6H_2O$ [1].

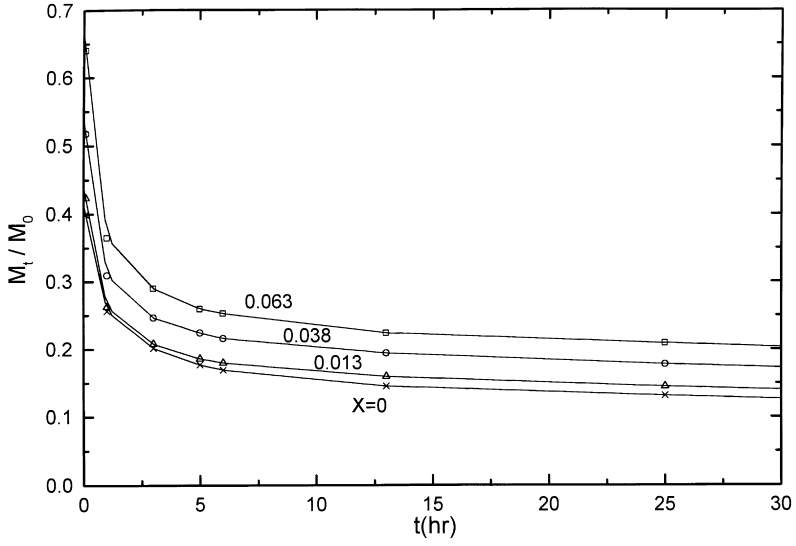

Fig. 4. Contents of solvent mixture at different concentrations of $FeCl_3 \cdot 6H_2O$ in specimens as functions of desorption time.

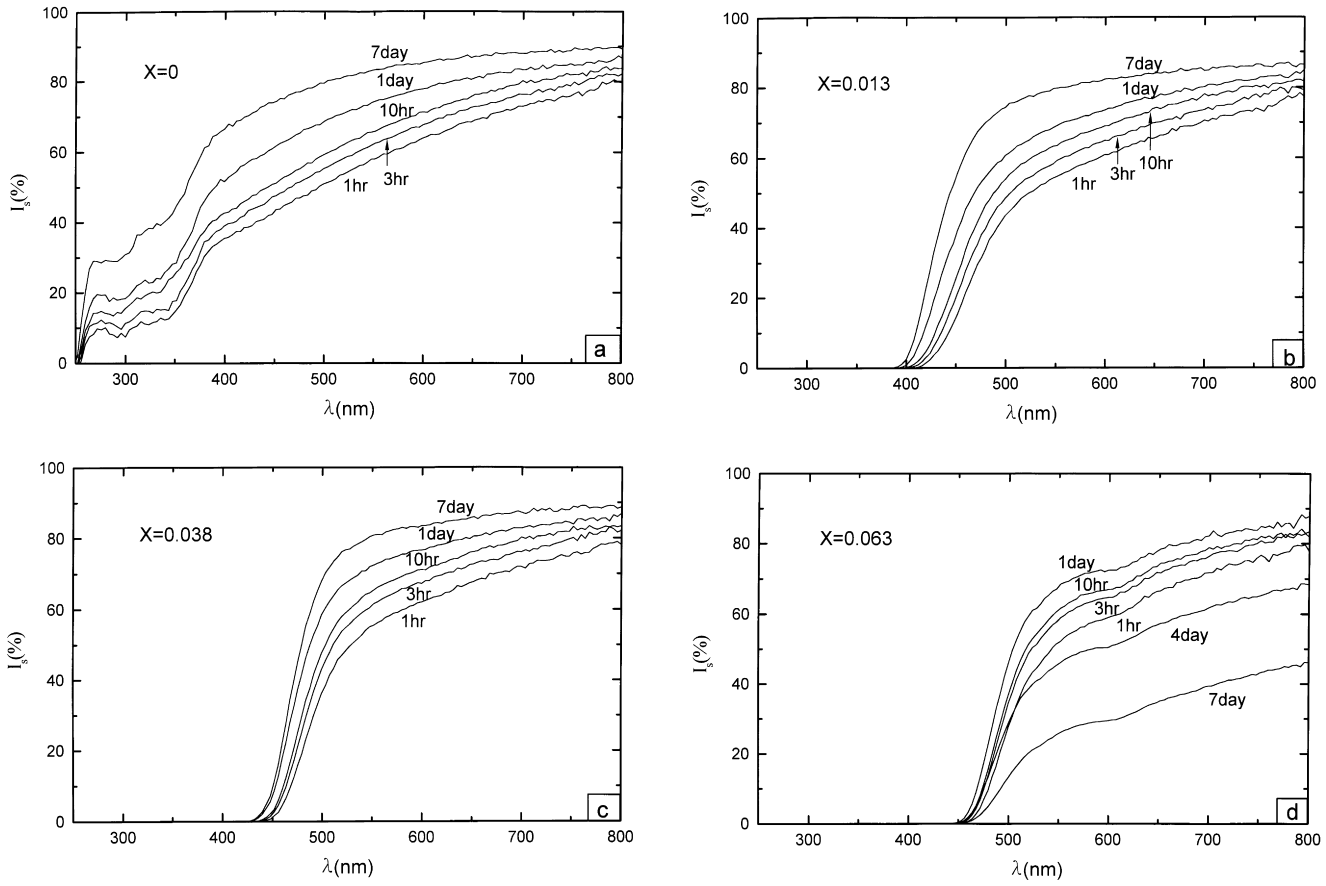

Fig. 5. The transmission spectrum of the specimens treated with solvent mixture of different concentrations of $FeCl_3 \cdot 6H_2O$ at 50°C after desorption for different periods: (a) $X = 0$ g/g; (b) 0.013 g/g; (c) 0.038 g/g; (d) 0.063 g/g.

The transmittance of the solvent-treated specimen varies with the visible wavelength in the range of 400–800 nm shown in Fig. 2(b) by dashed lines. This phenomenon was first observed by Lin et al. [20], and they proposed that the variation of transmittance with visible wavelength is due to the size of holes smaller than the visible wavelength. The holes are enlarged by solvent during the solvent uptake and shrunken during desorption. If the solvent content is small during uptake, the hole would be close up after desorption, but if the solvent content exceeds a critical value, the hole would not be closed up. The shrinking rate of hole is proportional to the desorption rate, which is defined by the slope of the curve of weight loss versus time. The weight of residual solvent in specimen during desorption is shown in Fig. 4 where M_0 is the weight of virgin PMMA. The solvent content in the specimen after desorption for 1 h lost more than 40 wt.% of saturated solvent. The rate of desorption becomes slow after 1 h and the shrinking rate of hole would also be slow. Therefore, the time dependence of transmittance in the visible wavelength after desorption for 1 h is shown in Fig.5(a)–(d). The scattering intensity, I_s, is defined as the difference of transmittance between the virgin specimen, I_0, and the desorbed specimen, I, at time $t = t_d$ where t_d is the desorption time. Note that we neglect the optical absorption. From Fig. 5, the scattering intensity of PMMA specimen with different concentrations of $FeCl_3 \cdot 6H_2O$ can be curve-fitted by the following equation:

$$I_s = a\lambda^{-n} \tag{7}$$

where a and n are constants. Both parameters, a and n, are calculated using Eq. (7) and listed in Table 4. The exponent, n, is in the range from 1.2 to 3.26. It increases with increasing desorption time for $t_d \leq 7$ days and $X \leq 0.038$ g/g and/or $t_d \leq 1$ day and $X = 0.063$ g/g. For a given desorption time, the exponent increases with increasing X in the

Table 4
Values of constant a, and exponent n in Eq. (7) related to the desorption time t_d and content of $FeCl_3 \cdot 6H_2O$

X (g/g)	Solvent		PMMA after desorption for t_d							
			$t_d = 1$ h		3 h		1 day		7 days	
	a	n	a	n	a	n	a	n	a	n
0	–	–	5.28	2.08	5.62	2.23	5.81	2.36	6.03	2.53
0.013	1.92	1.15	5.31	2.08	5.78	2.28	5.89	2.36	6.31	2.59
0.038	3.63	1.61	5.83	2.27	6.11	2.40	6.27	2.52	6.41	2.64
0.063	4.77	1.91	7.15	2.73	8.14	3.11	8.38	3.25	2.65	1.02

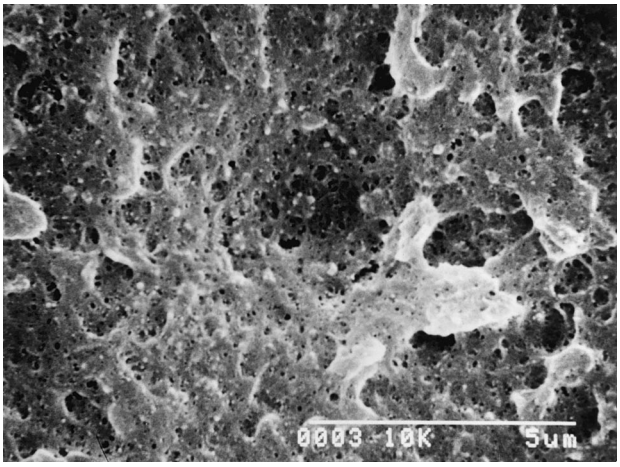

Fig. 6. The morphology of the specimen treated with solvent mixture of $X = 0.063$ g/g at 50°C observed by scanning electron microscope.

range $X \leq 0.038$ g/g. According to Rayleigh [19], the scattering intensity is proportional to the square of electric field arising from the particle, whose size is smaller than the visible wavelength. The electric field due to particle scattering is inversely proportional to the square of visible wavelength when the surface of particle is considered. Note that the surface dimension of particle is 2. Therefore, the scattering intensity is proportional to λ^{-4}, i.e. the exponent is 4 for Rayleigh scattering (or surface scattering). We assume that a hole is a particle and its surface dimension is of a fraction, not an integer. The exponent, n, smaller than 4 is believed due to the fractal of holes [25–27]. The fractal surface dimension of a hole is $n/2$. It is also found that the size of hole increases with increasing desorption time and increasing concentration of $FeCl_3 \cdot 6H_2O$. The scattering intensity of methanol mixed with different concentrations of $FeCl_3 \cdot 6H_2O$ also satisfies Eq. (7) and their parameters, a and n, are calculated and listed in Table 4. It is found that the value of n increases with increasing X. Note that n is equal to zero for pure methanol because the transmittance is independent of visible wavelength in the range of 400–700 nm. The fractal behavior of light scattering due to solvent mixture in PMMA will be investigated in the near future.

From the previous paragraph, the holes in the polymer are considered as small particles to scatter the visible light. A large number of holes in a specimen with solvent of $X = 0.063$ g/g at 50°C is shown in Fig. 6. The size of

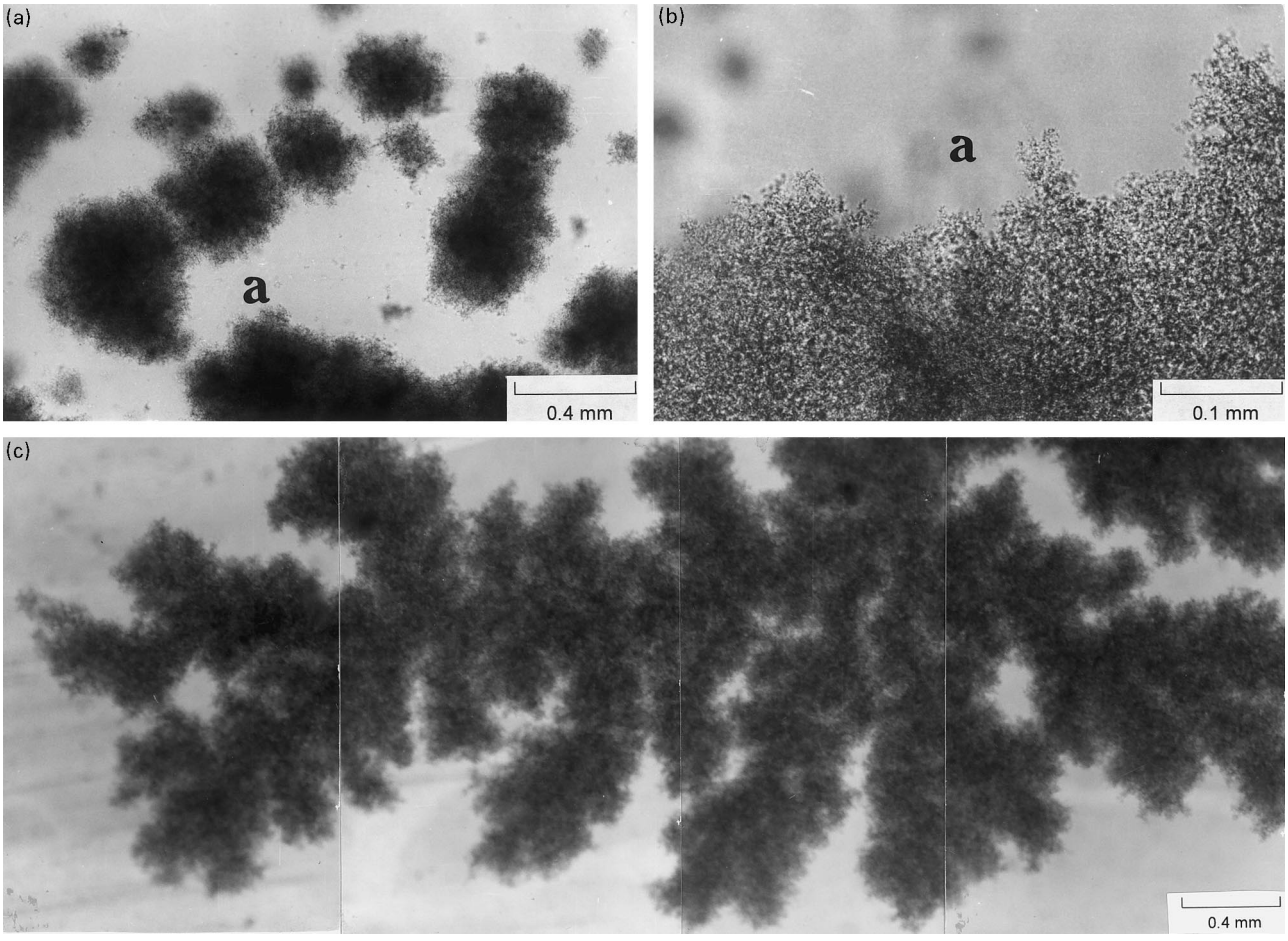

Fig. 7. Photographs of the opaque region of a specimen treated with solvent mixture of $X = 0.063$ g/g at 50°C: (a) after desorption for 4 days; (b) amplification of zone **a** in (a), and (c) after desorption for 7 days.

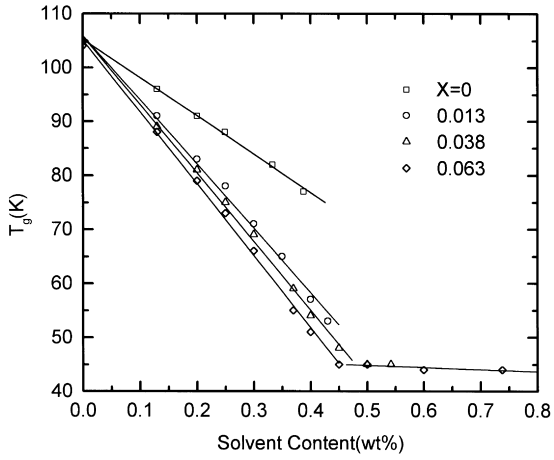

Fig. 8. Glass transition temperature (T_g) of desorbed specimens as a function of solvent content (wt.%).

holes varies from 30 to 300 nm. Rayleigh [19] suggested that the dependence of scattering intensity upon light wavelength arise from the different obstructive efficiency of the small particle to various light wavelengths. It is known that methanol and virgin PMMA are transparent in the visible range, i.e. transmittance is above 90%. For the specimen treated with methanol, the dependence of scattering intensity upon visible wavelength is only attributable to the holes. However, the situation for the specimen treated with the solvent mixture of $FeCl_3 \cdot 6H_2O$ and methanol becomes complicated. The solvent mixture itself exhibits the scattering behavior (see Fig. 2(a)) arising from the particles of metal coordinated complex in the solvent. Thus, for specimens treated with the solvent mixture, the relationship between transmittance and light wavelength is influenced not only by the presence of holes but also by the residual solvent in the specimen.

A special phenomenon is observed for the specimen treated with the solvent of $X = 0.063$ g/g and desorption time $t_d \geq 4$ days. The value of n is drastically reduced below 2 after desorption for 4 days. An opaque region appears in the inner layer of the specimen. This opaque region in the specimen treated with solvent mixture for 4 days is shown in Fig. 7(a) and (b). Fig. 7(c) shows the optical microscopy of a specimen after desorbed for 7 days. No hole smaller than the visible wavelength is observed in Fig. 7. The opaque region looks like clouds, and extends outward from the center of the specimen to the outer surface in the form of tree branch as a fractal cluster does [26,27].

The thermal analysis is helpful to understand the chain movement and the process of the creation of holes caused by mass transport. Glass transition temperature, T_g, can be regarded as an index of the chain mobility. Fig. 8 illustrates the change of T_g with solvent content. It is found that T_g decreases linearly from 104 to 77°C with increasing methanol content. Because the operating temperature (50°C) is below T_g through the whole transport process, the chain movement caused by the penetrated solvent is restricted in a small scale. As the specimen is removed from the water bath, the solvent moves from the interior and is escaped at the outer surface. When the solvent in the inner layer moves outward, the space previously occupied by the solvent becomes a hole. Thus the hole is smaller near the surface layer than in the interior. The morphology of cross-section of the specimen after desorption is shown in Fig.9(a)–(c). It can be seen from Fig. 9 that the microstructure changes from transparent to opaque via branches of trees when the concentration of $FeCl_3 \cdot 6H_2O$ is increased. The inner layer can be easily distinguished from the outer layer. The density of holes increases with increasing concentration of $FeCl_3 \cdot 6H_2O$ (not shown in Fig. 9).

Ferric chloride hexahydrate raises the affinity between solvent and polymer chains. The mobility of the polymer chain or T_g is sensitive to the solvent content (see Fig. 8). Therefore, the glass transition temperature of PMMA is lowered due to solvent uptake. The difference of glass transition temperature between the specimen treated with the solvent mixture and pure methanol increases with increasing concentration of $FeCl_3 \cdot 6H_2O$ for the same solvent content. Furthermore, for the solvent mixture with $X \geq 0.038$ g/g, the glass transition temperature is possibly below the operating temperature (50°C). That is, the polymer chain can move a large distance and the capacity occupied by the solvent greatly increases. The size of the hole is proportional to the solvent content inside the hole. While the specimen with a large solvent content is cooled and desorbed in air, the outflow of solvent makes the shrinking of holes. The solvent in the interior of the specimen diffuses outward and the holes become smaller. The empty holes scatter the visible light so that an opaque region first appears at the center of the specimen. As the solvent continues to flow to the external surface, the hole-created region increases, and the opaque region grows during the desorbed period.

4. Summary and conclusions

The mass transport of methanol mixed with ferric chloride hexahydrate ($FeCl_3 \cdot 6H_2O$) in poly(methyl methacrylate) (PMMA) and the related optical properties have been investigated. The sorption of methanol mixed with ferric chloride hexahydrate of different concentrations, $X = 0.013$, 0.038 and 0.063 g/g in PMMA at 40–60°C is a process of anomalous diffusion. The experimental data of mass uptake is in excellent agreement with the theoretical model. The diffusion coefficient and velocity which characterize Case I and Case II transport, respectively, satisfy the Arrhenius equation. The activation energy of Case I transport decreases with increasing concentration of $FeCl_3 \cdot 6H_2O$ whereas the activation energy of Case II transport slightly increases with increasing concentration of $FeCl_3 \cdot 6H_2O$. The equilibrium solvent content satisfies the van't Hoff's plot and the mass transport is endothermic. Both heat of mixing

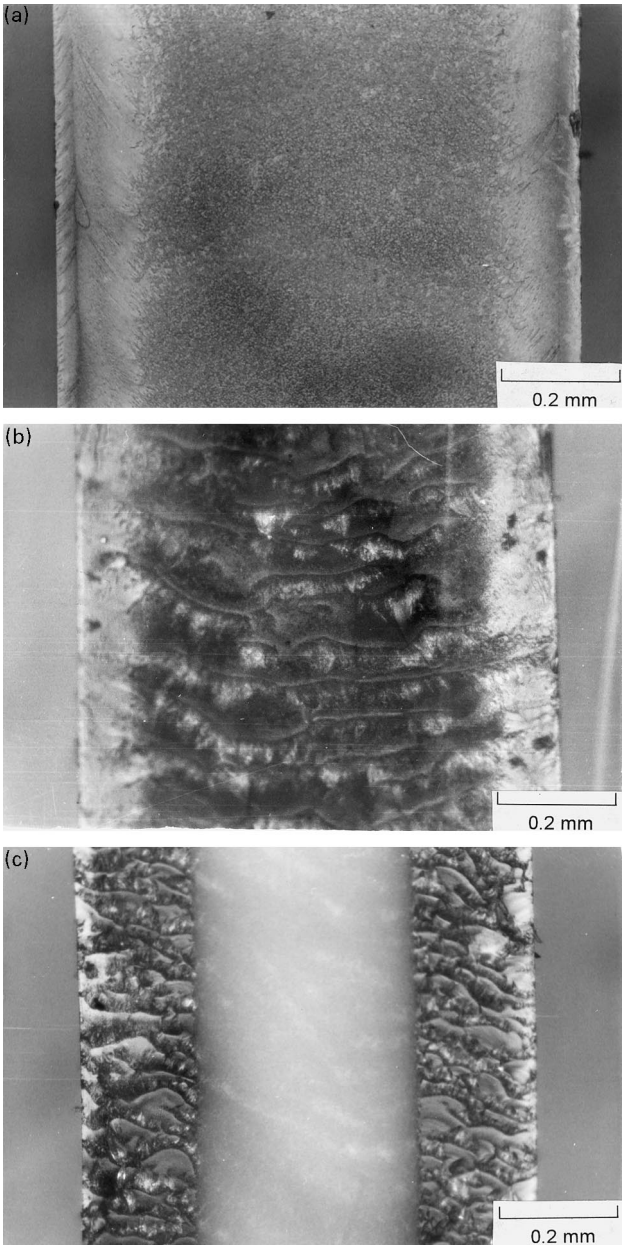

Fig. 9. The morphology of the cross-section of specimens treated with solvent mixture of different concentrations of $FeCl_3 \cdot 6H_2O$ at 50°C after desorption: (a) for $X = 0$; (b) for $X = 0.038$ g/g and (c) for $X = 0.063$ g/g.

and equilibrium solvent content increase with increasing concentration of $FeCl_3 \cdot 6H_2O$.

The cut-off wavelengths of solvent, PMMA specimens saturated with the solvent and desorption increase with increasing concentration of $FeCl_3 \cdot 6H_2O$, while the transmittance of solvent decreases with increasing concentration of $FeCl_3 \cdot 6H_2O$. For a given X, the transmittance of specimen increases with increasing desorption time and wavelength. The scattering intensity is inversely proportional to the wavelength of an exponent n which is in the range of 1.3–3.26 ($n = 4$ refers to the Rayleigh scattering). The visible wavelength dependence of light scattering occurs at the particle size smaller than the visible wavelength. Holes scatter the visible light and the SEM provides evidence of holes. The calculated value of n which is smaller than 4 implies that the hole has a fractal dimension. In addition to holes, the obstacle-like cloud also makes contributions to the dependence of scattering intensity of wavelength.

Acknowledgements

This work was supported by the National Science Council, Taiwan, Republic of China.

References

[1] Rabek JF, Lucki JB, Qu J, Shi WF. Macromolecules 1991;24:836.
[2] Tawansi A, Abdel-razek EM, Zidan HM. J Materials Sci 1997;32:6243.
[3] Rao TV, Chopra KL. Thin Solid Films 1979;60:387.
[4] Svorcik V, Kozlova JI, Rybka V, Hnatowicz V. Mat Lett 1995;23:321.
[5] Lindèn L, Rabek JF. J Appl Polym Sci 1993;50:1331.
[6] Stanke D, Halleusleben ML. Macromol Chem Phys 1995;196:1697.
[7] Mano V, Felisberti MI, Paoli MD. Macromolecules 1997;30:3026.
[8] Bailey JK, Brinker CJ, Mecavtney ML. J Colloid Interface Sci 1993;157:1.
[9] Kawai T, Nishihara H, Aamaki K. Corrosion Sci 1995;37:823.
[10] Vertes A, Nagy-Czako I, Burger K. J Phys Chem 1978;82:1469.
[11] Crank J. The mathematics of diffusion, 2nd. New York: Oxford University Press, 1975.
[12] Wang TT, Kwei TK, Frisch HL. J Polym Sci: Part A-2 1969;7:2019.
[13] Kwei TK, Wang TT, Zupko HM. Macromolecules 1972;5:645.
[14] Kwei TK, Zupko HM. J Polym Sci: Part A-2 1969;7:876.
[15] Wang TT, Kwei TK. Macromolecules 1973;6:919.
[16] Frisch HL, Wang TT, Kwei TK. J Polym Sci: Part A-2 1969;7:8.
[17] Harmon JP, Lee S, Li JCM. J Polym Sci: A Polym Chem Edn 1987;25:3215.
[18] Harmon JP, Lee S, Li JCM. Polymer 1988;29:1221.
[19] Jenkins FA, White HE. Fundamentals of optics. 2nd. New York: McGraw-Hill, 1950;22.
[20] Lin CB, Liu KS, Lee S. J Polym Sci: Part B: Polym Phys 1991;29:1457.
[21] Drago RS, Hart DM, Carlson RL. J Am Chem Soc 1965;87:1900.
[22] Collman JP, Hegedus LS, Norton JR, Finke RG. Principles and applications of organotransition metal chemistry, Mill Valley, CA: University Science Books, 1980.
[23] Aten WC. In: Whim BP, Johnson PG, editors. Directory of solvents, 2. Glasgow: Blackie, 1996. p. 10–47 chap. 2.
[24] Earnshaw A. The chemistry of transition elements, New York: Oxford University Press, 1973. p. 7–19.
[25] Wong P. Phys Today 1988;41:24.
[26] Feder J. Fractals, New York: Plenum Press, 1988.
[27] Vicsek T. Fractal growth phenomena, Singapore: Word Scientific Press, 1989.